MDPI

The Effect of Solvents on the Crystal Morphology of Pyriproxyfen

Xiaoyang Yan [1], Na Wang [1,*], Xiongtao Ji [1], Yaoguang Feng [1], Jun Li [1], Ting Wang [1], Xin Huang [1] and Hongxun Hao [1,2,*]

[1] National Engineering Research Center of Industrial Crystallization Technology, School of Chemical Engineering and Technology, Tianjin University, Tianjin 300072, China
[2] Collaborative Innovation Center of Chemical Science and Engineering (Tianjin), Tianjin 300072, China
* Correspondence: wangna224@tju.edu.cn (N.W.); hongxunhao@tju.edu.cn (H.H.)

Abstract: To obtain crystal products with ideal morphology and better quality, it is important to fully understand and grasp the affecting mechanism of solvents on crystal morphology. In this work, the interactions between solvent/solute molecules and different crystal faces of pyriproxyfen are investigated by a combination of experiments and molecular simulations. It is found that pyriproxyfen crystals grow into a lamellar morphology in methanol and ethanol, while the crystal grows into a three-dimensional shuttle morphology in n-butanol and n-heptane. Molecular simulations reveal that the molecular arrangement of crystal faces makes the alcohol hydroxyl adsorption sites exposed in different degrees, and the (002) face is more sensitive to alcohol hydroxyl than other faces. The adsorption of alcohol hydroxyl groups hinders the growth of crystal planes, so (002) and (102) faces become the main crystal planes in methanol and ethanol, and the lamellar crystal is formed. The developed knowledge of the growth mechanism based on the interaction between the solvent and crystal interface can be conducive to the further optimization of the pyriproxyfen crystal products.

Keywords: crystallization; crystal morphology; pyriproxyfen; molecular simulations

1. Introduction

The effect of solvents on crystal size and morphology is of great interest in crystal engineering. In pharmaceutical applications, the needle and lamellar morphology might be undesirable as the characteristics of easy agglomeration could affect downstream processing and reduce the product quality [1–3]. Solution crystallization is a commonly used process for purifying and refining pharmaceutical crystal products. The solvents may affect the polymorphism and morphology of crystals. The interaction between crystal faces and solvents can strongly impact (promote, inhibit, or even stop) the further outgrowth of individual crystal faces, thus changing the crystal morphology. Therefore, it is important to understand the mechanism of crystal morphology regulation in solution crystallization.

Generally, the morphology is one of the most critical factors reflecting product quality, which can affect product properties such as bulk density and fluidity, and further impact downstream processing such as filtration, tabletting, storage, and transportation. The morphology and size of crystalline materials can be influenced by different solvents or characteristic additives [4–9]. Hatcher et al. [4] studied the additive crystallization routes to control the crystal morphology of lovastatin and they found that the inclusion of non-size-matched polymer additives can obviously change the crystal morphology. Wu et al. [10] studied the effect of additives on different crystal faces of p-toluamide, and found that different additives could selectively promote the growth of specific crystal faces. Zhang et al. [11] studied the morphologies of HMX in acetone and dimethyl sulfoxide (DMSO) using the single-crystal X-ray diffraction (SCXRD). It was found that the DMSO can significantly decrease the growth rate of the (110) and (101) planes of the HMX crystal

compared to acetone. The structural characteristics of the crystal faces are the main reasons for the growth behaviors [12,13]. Civati et al. [14] analyzed the intermolecular interactions in known needle structures from the literature, and divided the needle-like crystals into persistent and controllable needle formers by whether the morphology can be controlled by the choice of solvent. Liu et al. [15] investigated the crystal faces growth "dead zone" phenomenon, and suggested that the behavior is linked to molecular-scale surface roughness. Computer simulation and the establishment of different growth models bring more perspectives for understanding anisotropic crystal growth [16–18]. The molecular-level structure visualization can be provided by molecular simulation [13,19,20]. Song et al. [21] studied the crystal morphology of FOX-7 in dimethyl sulfoxide/water mixed solvent by molecular dynamics simulations, and explained the variation in crystal morphology caused by different external conditions. Liu et al. [22,23] found the solvent adsorption sites at the HMX crystal face by molecular simulation and proposed that the binding energy of the solvent adsorption sites is the critical factor to morphology prediction. Although the previous studies have made great progress, the underlying mechanism of solvents on the growth of organic crystals is still not fully revealed. Thus, it is essential to further investigate the affecting mechanism of solvents on crystal growth and morphology.

Pyriproxyfen is a new type of insecticide of a juvenile hormone, which is mainly used to control multiple insects with the advantages of low toxicity and high efficiency [24,25] and crystallization is one of the important unit operations in the production of pyriproxyfen, which can significantly affect its structure, morphology, crystal particle size, etc. Generally, lamellar crystals are more likely to break and aggregate than block-like crystals, and further lead to the inclusion of impurities in the product and reduce product quality. This could also seriously reduce the insecticidal efficacy of pyriproxyfen. Therefore, it is necessary to explore effective approaches to regulate the crystal morphology of pyriproxyfen. In this work, pyriproxyfen was crystallized in different solvents (methanol, ethanol, n-propanol, n-butanol, and n-heptane) to investigate the effect of solvents on crystal habits. Molecular dynamics simulation and interfacial structure analysis were used to investigate the adsorption sites of alcohol hydroxyl groups on corresponding crystal planes and the effect of crystal plane structure on solvent sensitivity. The results presented in this work can help to design the crystallization process for obtaining better pyriproxyfen crystal products.

2. Experiment

2.1. Materials and Characterization

Analytically pure pyriproxyfen (99%, $C_{20}H_{19}NO_3$, CAS Registry No. 95737-68-1) was purchased from Heowns Biochem LLC and was used without further purification. N-heptane (AR) was purchased from Kemiou Chemical Reagent Co., Ltd (Tianjin, China). Methanol (AR), ethanol (AR), n-butanol (AR), and n-propanol (AR) were all purchased from Jiangtian Chemical Technology Co., Ltd (Tianjin, China). All reagents were used as received.

Powder X-ray diffraction was used to detect the crystal form of pyriproxyfen after each experiment to determine whether the difference in crystal morphology is caused by polymorphism. Powder X-ray diffraction (PXRD, D/MAX-2500, Japan) was measured using Cu Kα radiation (1.5405 Å) with an electric current of 100 mA and voltage of 40 kV. The step size was 0.02° and the scanning rate was 8 °/min over diffraction angles (2θ) from 2° to 40°.

2.2. Crystallization Process

The crystal products were obtained by cooling crystallization from different solvents. A certain solution concentration of pyriproxyfen was prepared at 313 K with 150 rpm of stirring. Then, the solution was cooled down by using a water bath under 150 rpm of stirring to precipitate pyriproxyfen. The crystal products were filtered and dried at room temperature, and then collected for crystal form detection. The large shuttle crys-

tals of pyriproxyfen were gained by evaporative crystallization in n-heptane solution at room temperature.

2.3. Molecular Dynamics Simulation

The crystal structure file of pyriproxyfen was taken from CSD (Cambridge Structural Database) [26], which belongs to an orthorhombic system with lattice parameters a= 10.068 Å, b= 8.028 Å, and c= 40.913 Å. There are eight pyriproxyfen molecules in each unit cell and the molecular and unit cell structures of pyriproxyfen are shown in Figure 1.
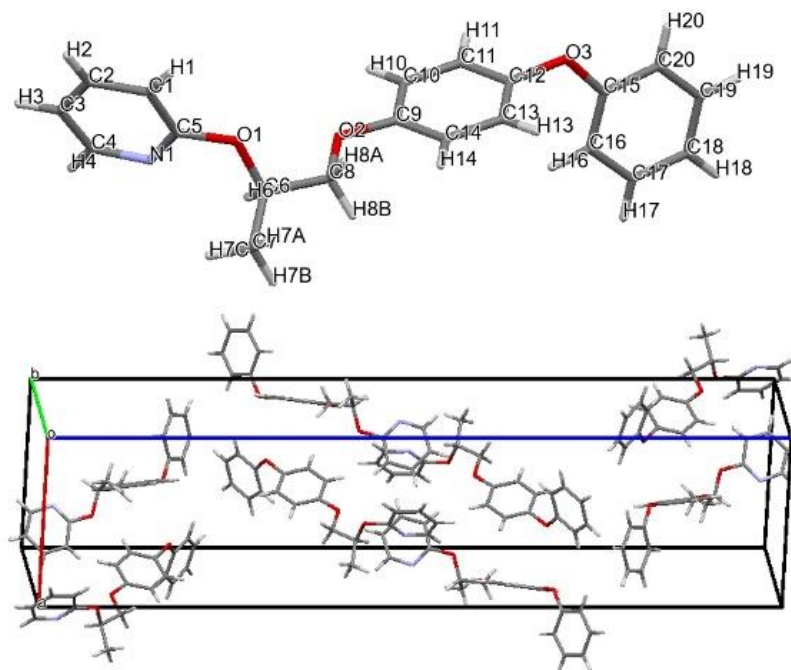

Figure 1. Molecular structure and lattice structure of pyriproxyfen. The crystal structure of pyriproxyfen was taken from CSD [26].

All computation simulations were performed using Materials Studio 7.0. Geometry optimization and molecular dynamics (MD) simulation were performed with the Forcite module with the COMPASS (condensed phase optimized molecular potentials for atomistic simulation studies) [27] force field.

The system of solvent crystal interaction consists of three main parts: crystal face, solution region, and the interface between crystal and solution. In order to explore the impact of the interaction of the three parts at the molecular level, appropriate models were constructed. The model of the crystal surface growth system contains three parts: crystal layer, solution layer, and a vacuum layer to eliminate the effect of additional free boundaries. For the crystal layer, the length and width of the crystal layer were selected to be at least greater than 30 Å [28], and were verified by the model size convergence.

For the solution layer, in order to find the influence of solvent on the adhesion of solute molecules on the crystal surface, a series of periodic pure solvent boxes and solution boxes were constructed, as shown in Figure 2. The length and width of these amorphous cells were as large as the U and V of the supercells of crystal layers, respectively. The solvent molecules as well as solute molecules were also geometrically optimized with the same force field. In the pure solvent model, the periodic solvent boxes were constructed in the amorphous cell module and then added to the crystal layer. In the solution model, the same number of solute molecules were added to the solution model, and solvent molecules were added to make the solution layers of different solutions equal in height. For the crystal layer, the crystal layer was fixed completely to reflect the crystal structure realistically in the crystal plane fixation model. In the crystal plane partly fixed model, the part of

the crystal phase supercell away from crystal–solvent interface was fixed, and the 1.5-molecules thickness of the corresponding crystal plane near the solvent layer could move freely (Figure 2). It reflects the solvation of the crystal surface in solution. As shown in Figure 2, combining the solution layer and the crystal layer, a double-layer crystal–solvent interface model was finally established, and a 70 Å thick vacuum layer was built above the solvent layer to eliminate the effect of additional free boundaries. For the convenience of description, different models were marked with the following codes. PS-CF is the model combined with the pure solvent box and the completely fixed crystal layer. PS-PF is the model combined with the pure solvent box and the partly fixed crystal layer. CS-CF is the model combined with the solution box and the completely fixed crystal layer, and CS-PF is the model combined with the solution box and the partly fixed crystal layer.
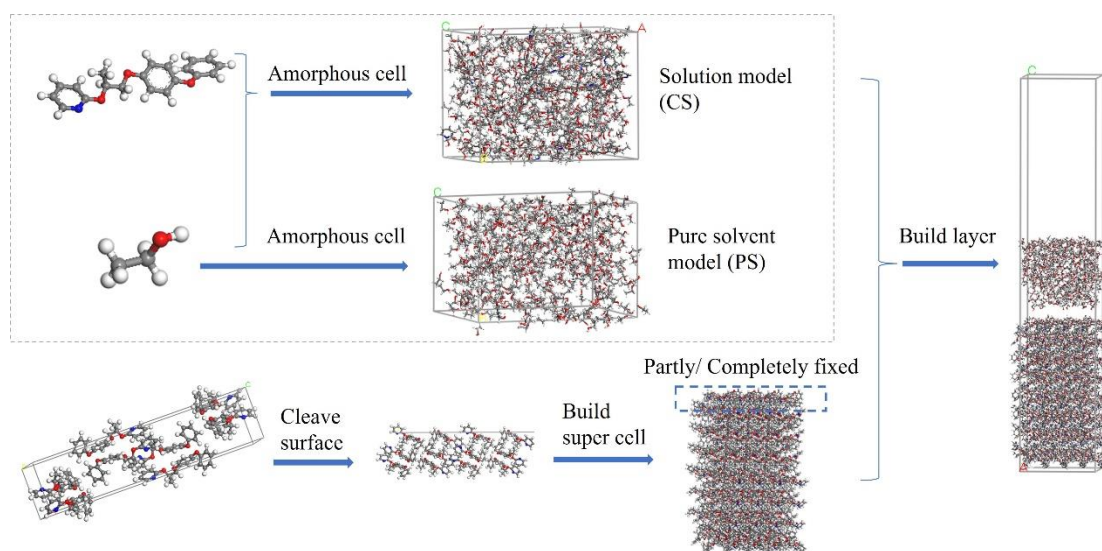

Figure 2. Schematic diagram of the construction of the model.

After establishing the periodic models, all the models were optimized using the Forcite module to eliminate irrelevant contacts with the Smart approach, and all the structures could converge within 1 million steps. The NHL thermostat was used to control the temperature at 298 K, and NVT ensemble MD simulation was performed to ensure the system was well-relaxed. Then, the optimized model was set to NVT mode for the 700 ps dynamic process with a timestep of 1 fs. Radial distribution function (RDF) analysis and energy analysis were performed using the last 200 ps of energy stability.

E_{int} is the interaction energy between the solution and crystal faces, and its calculation formula is as follows:

$$E_{int} = E_{tot} - (E_{cry} + E_{sol}) \tag{1}$$

where E_{tot} is the total energy of the solvent layer and crystal surface layer in the two-layer model, E_{cry} is the energy of the crystal surface layer, and E_{sol} is the energy of the solvent layer.

The electrostatic forces were evaluated by Ewald's method with an accuracy of 0.0001 kcal mol^{-1} and the van der Waals interactions were calculated by an atom-based method with a cut-off distance of 15.5 Å respectively.

3. Results and discussion

3.1. Identification of Polymorph and Morphology in Different Solutions

The morphology of pyriproxyfen crystals grown in different solvent systems is shown in Figure 3. The crystals grown in ethanol (Figure 3d) and methanol (Figure 3a,c) solution have a lamellar morphology. As the polarity of solvent molecules decreases, the crystals

grown in n-propanol (Figure 3e) gradually tend to a shuttle shape, and the crystals grown in n-butanol (Figure 3f) and heptane (Figure 3g) become more stereoscopic shuttle crystals.
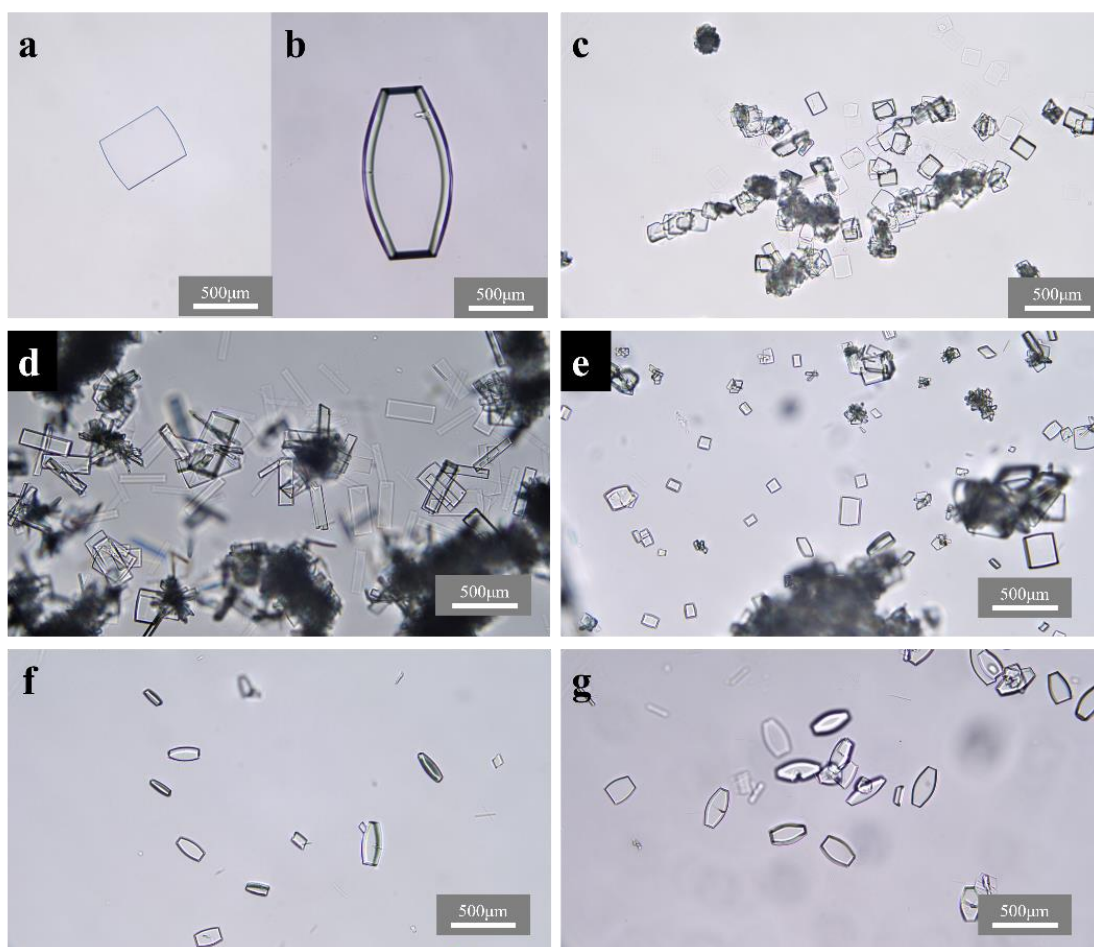

Figure 3. (**a**) Pyriproxyfen crystal with lamellar shape in ethanol; (**b**) pyriproxyfen crystal with shuttle shape in heptane; pyriproxyfen crystal grown in (**c**) methanol, (**d**) ethanol, (**e**) N-propanol, (**f**) N-butanol, and (**g**) heptane.

The solvent may change the crystal form of the drug [29], so the obtained pyriproxyfen crystal products were characterized by XRD to determine their crystal form. Figure 4 shows the powder XRD spectra of the crystal product of pyriproxyfen obtained in different solvents and the simulation XRD data of the pyriproxyfen crystal form reported by Kang et al. [26]. It can be seen that the positions of characteristic peaks of the crystal products obtained from recrystallization in various solvents are the same, and the characteristic peaks of the XRD diagrams of the pyriproxyfen crystals obtained in various solvents are also consistent with the simulated spectra. Thus, no polymorphic transformation takes place, and crystal forms of all the samples are consistent with the reported crystal form.
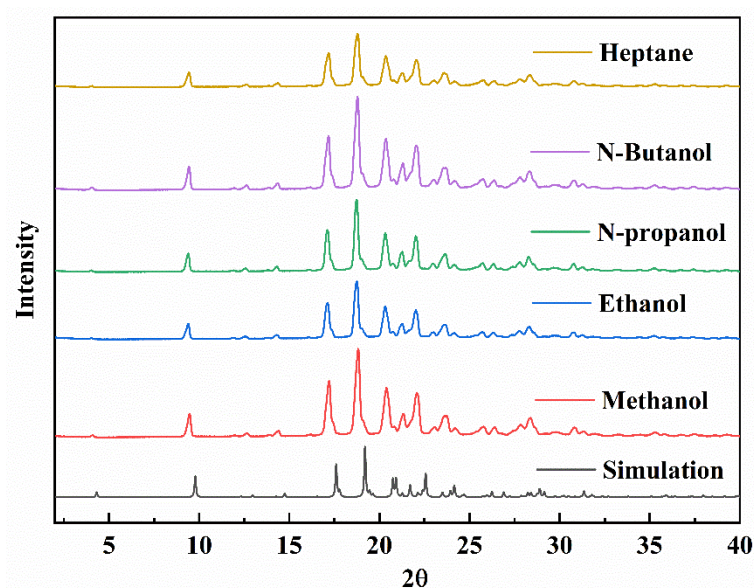
Figure 4. XRD patterns of the pyriproxyfen crystals obtained from different solvents and simulated by single crystal structure (CCDC number: 1412612).

　　The Attachment Energy (AE) model was proposed by Hartman and Bennema, which is commonly used to predict crystal morphology [30]. The attachment energy (E_{att}) is defined as the energy released on the attachment of a growth slice to a growing crystal surface, and the crystal face with a more negative attachment energy would have a faster relative growth rate. The main crystal faces predicted in vacuum by the AE method is presented in Table 1 and Figure 4a. Under vacuum conditions, there are three main planes, namely (002), (102), and (111), and the proportion of crystal face area is 60.2%, 19.1%, and 20.6%, respectively, as shown in Table 1. From Table 1, it can be seen that the (111) crystal plane has the largest |E_{att}| value compared with the (002) crystal plane and (102) crystal plane and, hence, it is considered that the (002) crystal plane and (102) crystal plane are more stable. Moreover, in the actual solution, as shown in Figures 3 and 5, the (002) and (102) crystal planes are the most important crystal planes in lamellar crystals. The largest crystal plane of the pyriproxyfen crystal grown in ethanol solution is the (002) crystal plane, while the (002) plane of pyriproxyfen obtained in n-heptane does not occupy the best morphological position as that in ethanol solution. With the influence of n-heptane, the shuttle crystal expands to form a block, which is less likely to break and coalesce than two-dimensional flakes.

Table 1. Crystal habit value of pyriproxyfen under vacuum conditions.

(h k l)	d_{hkl} (Å)	Surface Area (Å^2)	Total Facet Area%	E_{att} (kcal mol^{-1})
(002)	20.135	78.566	60.2	−43.779
(102)	8.425	375.530	19.1	−117.168
(111)	6.181	511.909	20.6	−182.490

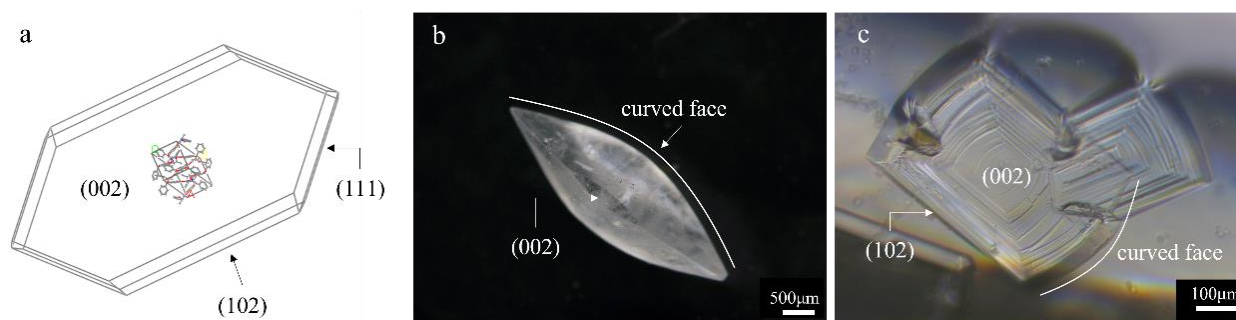**Figure 5.** (**a**) The main crystal faces of pyriproxyfen predicted in vacuum; (**b**) pyriproxyfen crystal grown in heptane solution; (**c**) pyriproxyfen crystal grown in ethanol solution.

The curved surface is the most important crystal surface of the shuttle crystal formed in heptane solution, and the lamellar crystals formed in ethanol solution also have a curved edge. This curved surface and curved edge are composed of a crystal plane group represented by the (111) plane.

3.2. Effect of Solvent on the Interactions between Solute Molecule and Crystal Plane

In order to understand the influence of different solvents on the crystal morphology of pyriproxyfen, molecular dynamics simulation was used to investigate the interactions between the crystal surface and solution layer.

The radial distribution function (RDF) usually refers to the distribution probability of other particles in space (how far away from a given particle) given the coordinates of a particle. Therefore, the RDF can be used to study the properties of the interactions between atoms by quantifying the distribution of the surrounding atoms with the designated atom as the center. Generally, the position of the peak marks the type of interaction: the hydrogen bonding interaction distance is around 3.1 Å, and the van der Waals interaction distance ranges from 3.1 to 5 Å. The height of the peak also represents the intensity of the interaction. RDF images of N atoms on solute pyriproxyfen versus the whole crystal surface layer were calculated and the results are shown in Figure 6.
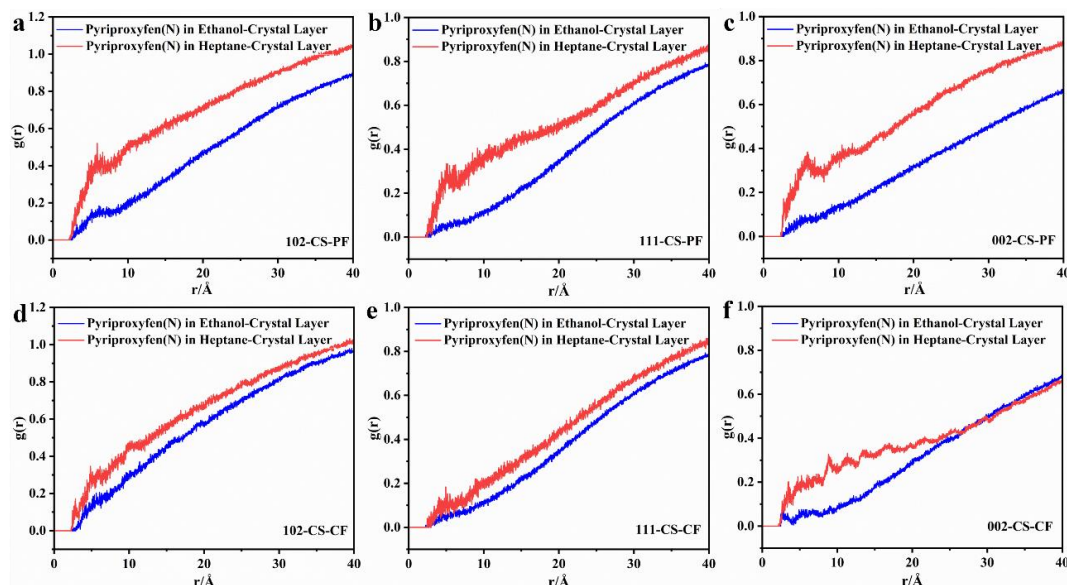

Figure 6. RDFs of the solute pyriproxyfen (N) to crystal layer in different solution environments. (**a**–**c**) The models with partly relaxed crystal layer in (102) face, (111) face, and (002) face, respectively. (**d**–**f**) The models with completely fixed crystal layer in (102) face, (111) face, and (002) face, respectively.

Take the (102) crystal face as an example. Figure 6a,d show the radial distribution function between N atoms on pyriproxyfen (solute molecules) and the (102) crystal plane. Figure 6a shows the molecular partial fixation model on the crystal layer of the (102) crystal plane and Figure 6d shows the model of complete molecular fixation on the (102) crystal plane. The red line is the result in the n-heptane system, and the blue line is the result in ethanol solution. It can be seen from Figure 6a,d that the RDF graph line of the interaction between the pyriproxyfen molecule and the crystal plane has a peak at about 5 Å, which represents the van der Waals interaction between the pyriproxyfen molecule and (102) crystal plane. In Figure 6a,d, the peak intensity of the red line obtained in the n-heptane system is higher than that of the blue line obtained in the ethanol system, which indicates that in the n-heptane system, the interaction between pyriproxyfen (solute) and the crystal plane is stronger, while in the ethanol system, the interaction between the pyriproxyfen molecule and the crystal plane is shielded. In Figure 6a, the peak intensity value between the red line and the blue line is significantly greater than that in Figure 6d. It means that when the molecules on the surface layer of the crystal are not fixed, the solvent has a greater influence on the solute crystal surface interaction. Figure 6b,e show the RDF on the (111) crystal plane, and Figure 6c,f show the RDF calculation results on the (002) crystal plane. They show similar results as the (102) crystal plane in different solvents.

3.3. Adsorption of Ethanol on Main Crystal Planes

The adsorption of alcohol hydroxyl groups on each crystal plane of pyriproxyfen was studied with ethanol solvent as the representative. Generally, a smaller *r* and a higher peak mean a stronger interaction. As shown in Figure 7a, the RDFs of pyriproxyfen (H4) and ethanol (O) show the highest intensity (the atomic label is consistent with that marked in Figure 1). It indicates that the pyriproxyfen (H4) has the strongest hydrogen bonding with ethanol (O). As shown in Figure 7b, the RDFs of ethanol (O) and pyriproxyfen (H4) is still the highest, which indicates that the adsorption of ethanol molecules on the (002) crystal plane is mainly caused by the hydrogen bonding interaction between ethanol (O) and the pyriproxyfen (H4). Similarly, the hydrogen bonding interaction between pyriproxyfen (O3) and ethanol (H) mainly causes the adsorption of ethanol molecules on the (102) crystal plane (Figure 7c). The adsorption of ethanol on the (111) crystal plane is caused by the interaction of pyriproxyfen (O3)-ethanol (H) and ethanol (O)-pyriproxyfen (H4) (Figure 7d). It can be seen that the g(r) of ethanol on different crystal faces is: (002) > (102) > (111) (see Figure 7b–d), which means that the growth of (002) and (102) is more significantly inhibited.

In ethanol solution, due to the strong hydrogen bonding interaction, the ethanol molecules can be attracted to the crystal surface easily. The close contact between ethanol and the crystal face makes the pyriproxyfen relatively far away. In n-heptane solution, without the strong influence of the solvent, the pyriproxyfen molecules are more easily attracted by the crystal plane.
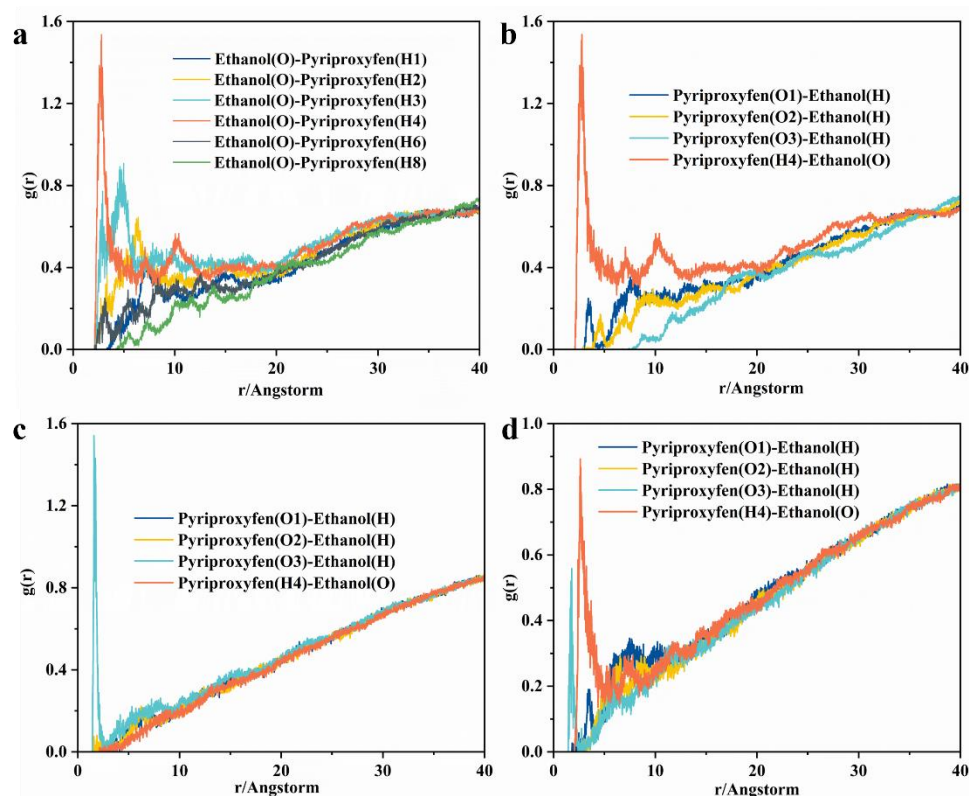
Figure 7. RDFs of pyriproxyfen in crystal layer and ethanol. (**a**) RDFs of the ethanol (O) to different pyriproxyfen (H) on (002) crystal layer; (**b**) RDFs of the ethanol around the interfacial layers of (002); (**c**) RDFs of the ethanol around the interfacial layers of (102); (**d**) RDFs of the ethanol around the interfacial layers of (111).

3.4. Structure Analysis of Main Crystal Planes

The different sensitivity of crystal faces to solvents is an important reason for the different morphology. We established models including two solvent systems (ethanol and n-heptane) to study the influence of solvent. The characteristics of the crystal face are the other important factors affecting the crystal growth morphology. Here, a model was established to explore the situation when the crystal plane is partially solvated in the solution (partly fixed in the crystal layer). According to 3.2, different solvents will affect the solute–crystal surface interactions. Therefore, a pure solvent model and a solution model were established to further understand the competitive adsorption of solute molecules and solvent molecules on different crystal planes.

Figure 8 shows the distribution of bond chains on the (102) crystal plane and (002) crystal plane. In Figure 8a, it can be seen that the (002) crystal plane is approximately parallel to the bond chain composed of N1-C2 and C1-H4 bonds, while the bond chain composed of H14-C18 and H19-C15 passes through the (002) crystal plane almost vertically. In Figure 8b, the (102) crystal plane is parallel to the bond chain composed of H14-C18 and H19-C15 bonds. The (102) crystal plane and (002) crystal plane are parallel to two different groups of bond chains. This result can explain why they are more stable.
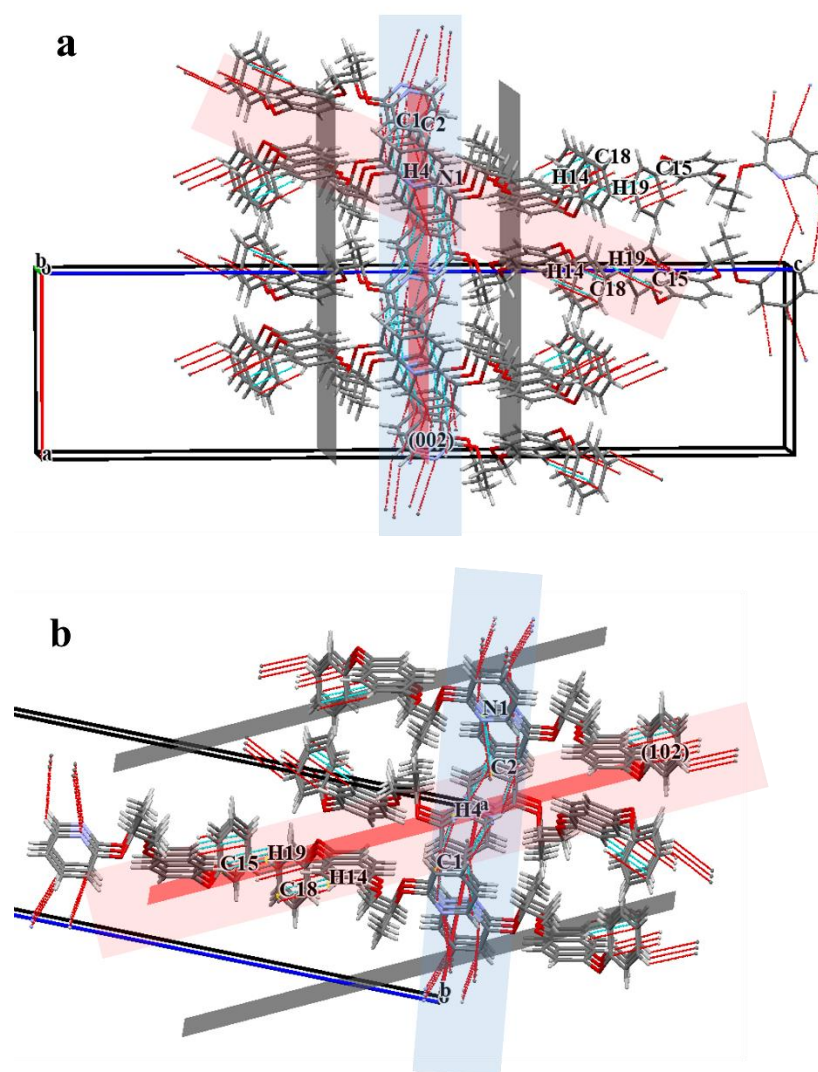
Figure 8. The bond chains (red and cyan short line) and crystal plane (red and gray plane) of pyriproxyfen crystal. (**a**) (002) face; (**b**) (102) face. The blue block is the bond chain composed of N1-C2 and C1-H4 bonds, and the red block is the bond chain composed of H14-C18 and H19-C15 bonds.

As shown in Figure 9a, the molecules of the (002) plane are approximately arranged in a vertical arrangement and, thus, a large amount of pyriproxyfen (H4) is exposed in the solution environment. In the (102) plane, the molecules are arranged in an inclined way, so the pyriproxyfen (O3) can be exposed easily. It is shown in Figure 9b that the position of pyriproxyfen (H4) is sandwiched between two molecules in a narrow space. It may cause the adsorption site to not easily contact with the solution. In the (111) face, the pyriproxyfen (O3) and pyriproxyfen (H4) are both exposed, and it has a rougher crystal plane than the (002) and (102) faces do.
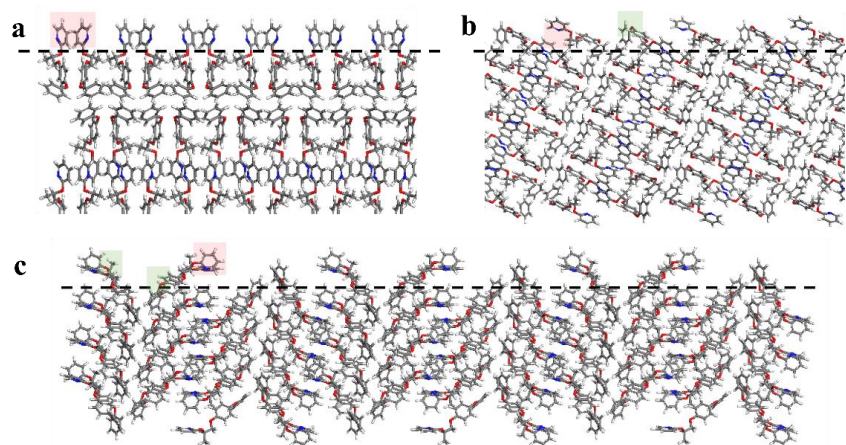
Figure 9. Surface structure of morphologically important (MI) faces of pyriproxyfen. (**a**) (002) face; (**b**) (102) face; (**c**) (111) face. The red block shows the position of H4 on pyriproxyfen, and the green block shows the position of O3 on pyriproxyfen.

3.5. Sensitivity of Different Crystal Faces to Ethanol Solvent

The influence of the solvent factor is reflected in each crystal plane in Figure 10 and Table 2. The binding energy E_b is defined as $|E_{int}|$. For the (002) crystal face, the E_{int} value of the interaction strength of the ethanol system is -337 kcal mol^{-1} and -423 kcal mol^{-1}, while that of the n-heptane system is -220 kcal mol^{-1} and -290 kcal mol^{-1}. It can be seen from Figure 10 that the E_b in the ethanol system is obviously stronger than that in the n-heptane system in different models, and the solvent is the largest factor affecting the (002) plane. The vertical pyriproxyfen on the (002) face exposes its sites of interaction with ethanol, which make the (002) face more easily inhibited by ethanol, as shown in Figure 9a. The adsorption of solvent molecules on the crystal surface inhibits the crystal surface growth [31–33]. Therefore, the (002) face of the pyriproxyfen crystal grown in n-heptane solution tends to disappear, while in ethanol solution, it becomes the most important crystal plane, as shown in Figures 5 and 11.
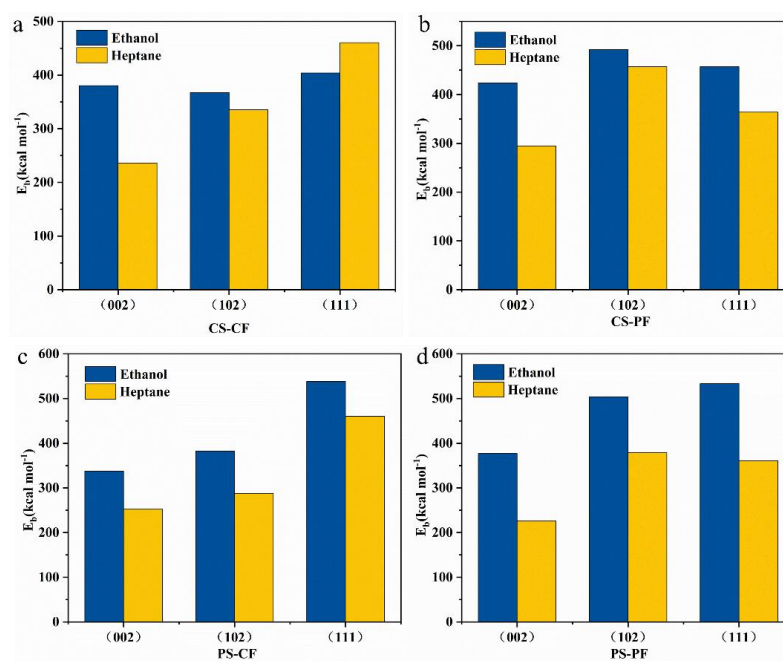

Figure 10. (**a**–**d**) The binding energies E_b (kcal mol^{-1}) between the crystal layer and solution layer of the (002), (102), and (111) crystal face in different models.

Table 2. The E_{int} (kcal mol^{-1}) between the crystal layer and solution layer of the (002), (102), and (111) crystal faces from different models.

Face	Solvent	E_{int} (kcal mol^{-1})			
		CS-CF	CS-PF	PS-CF	PS-PF
(002)	Ethanol	−380.3	−423.7	−337.3	−376.9
	Heptane	−236.2	−294.8	−252.2	−226.3
(102)	Ethanol	−367.4	−492.1	−381.9	−504.0
	Heptane	−335.2	−457.1	−287.7	−379.2
(111)	Ethanol	−403.9	−457.2	−538.2	−533.1
	Heptane	−460.2	−363.8	−460.2	−360.7
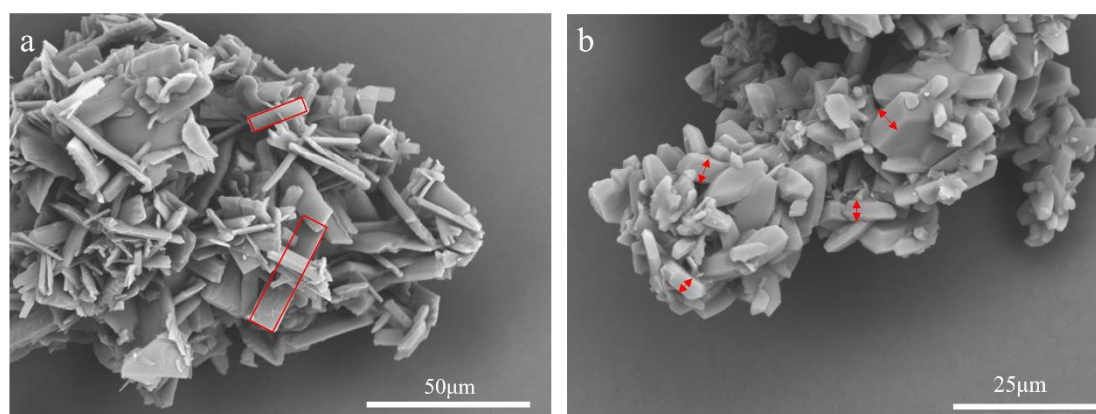
Figure 11. (**a**) The lamellar pyriproxyfen crystal obtained in ethanol solution; (**b**) the shuttle pyriproxyfen crystal obtained in n-heptane solution. The red square frame highlights the lamellar crystal of pyriproxyfen. The red line in b shows the thickness of the fusiform pyriproxyfen crystal.

For the (102) crystal plane, the E_{int} value of the interaction strength of the ethanol system is −367 kcal mol^{-1} and −503 kcal mol^{-1}, and it is −287 kcal mol^{-1} and −457 kcal mol^{-1} in the n-heptane system (Table 2). The crystal–solution interaction in the ethanol system is stronger than that in the heptane system in every model. In the n-heptane system, for the (102) face, the E_{int} values calculated in models PS-CF, PS-PF, CS-CF, and CS-PF are −287.662 kcal mol^{-1}, −379.223 kcal mol^{-1}, −335.202 kcal mol^{-1}, and −457.12 kcal mol^{-1}, respectively. The interaction strength in the solution model (CS) is stronger than that in the pure solvent model (PS), under the same crystal layer condition. This means that for the (102) crystal face, the adsorption between solute molecules and the crystal face is stronger than that between heptane molecules and the crystal face. Therefore, the growth promotion effect of n-heptane in the vicinity of the (102) crystal plane significantly affects the growth of the crystal plane, so it tends to disappear and form a shuttle shaped crystal.

The thickness of shuttle crystals is obviously thicker than that of lamellar crystals. This change in thickness is caused by the inhibition of the growth of the (002) crystal plane in ethanol solution, and the easier combination of the solute pyriproxyfen and crystal plane in n-heptane solution. The adsorption of ethanol on the (102) crystal surface is also greater than that of heptane, so the (102) crystal surface is inhibited in ethanol solution, thus causing the experimental results shown in Figures 5 and 11.

For the (111) crystal face, the hydrogen bonding interaction between ethanol and (111) is not as strong as those in (002) and (102) faces. As is shown in Figure 10, the influence of different solvent systems on the (111) crystal plane is not as strong as that on (002). The (111) face has an obvious ripple structure, while the (102) and (002) faces are relatively smooth (Figure 9). The rough crystal surface is conducive to the adsorption of different solvent molecules and solute molecules. Therefore, the sensitivity of the crystal face to ethanol is (002) > (102) > (111). With the (002) face more inhibited in ethanol while the

(102) face is more promoted in n-heptane, the pyriproxyfen crystal grows into a lamellar morphology in ethanol and becomes more stereoscopic shuttle crystals in n-heptane.

4. Conclusions

In this work, the influence of different solvents on pyriproxyfen crystal morphology was investigated. With the increase in carbon chains of the alcohol solvent, the morphology of pyriproxyfen in the alcohol solvent changes from a lamellar morphology to more stereoscopic shuttle crystals. The (102) and (002) faces are the main crystal plane of pyriproxyfen and the (111) face represents the curved surface. MD simulations and crystal plane structure analysis were carried out to explore the mechanism underlying the effect of solvent on the crystal growth. Different models were established to explore the influence of solvent on each crystal plane, and the competitive adsorption of solvent molecules and solute molecules on each crystal plane. It was found that the pyriproxyfen molecules (solute) in n-heptane solution show a closer interaction with the crystal surface than that in ethanol, and the (002) crystal face has the strongest sensitivity to alcohol hydroxyl. The interaction between ethanol and the crystal face is analyzed by calculating the g(r) on the main crystal faces. It was found that it is easy for the hydroxy-O of ethanol to generate hydrogen bonding interaction with the H4 of the pyriproxyfen molecule on the (002) and (111) plane, and it is easy for the hydroxyl-H to generate H bond interaction with the O3 of the pyriproxyfen molecule on the (102) and (111) planes. The (002) face is characterized by vertically arranged pyriproxyfen molecules with the exposure of the pyridine group, which can easily combine with alcohol hydroxyl, so the growth of the (002) crystal plane is inhibited in the ethanol solution. These results are consistent with the experimental observations. The influence of solution environment on solute molecule–crystal plane interaction, the adsorption of solvent molecules on the crystal plane, and the influence of crystal plane structure jointly contribute to the change in crystal morphology in different solution environments.

Author Contributions: Conceptualization, X.Y. and N.W.; formal analysis, X.Y., Y.F., J.L., T.W. and X.H.; funding acquisition, T.W., X.H. and H.H.; investigation, X.Y., N.W., X.J., T.W. and X.H.; methodology, X.Y., N.W. and X.J.; project administration, N.W. and H.H.; writing—-original draft, X.Y.; writing—-review and editing, N.W. and H.H. All authors have read and agreed to the published version of the manuscript.

Data Availability Statement: Data available on request due to restrictions.

Conflicts of Interest: There are no conflicts to declare.

References

1. Puel, F.; Verdurand, E.; Taulelle, P.; Bebon, C.; Colson, D.; Klein, J.P.; Veesler, S. Crystallization mechanisms of acicular crystals. *J. Cryst. Growth* **2008**, *310*, 110–115. [CrossRef]
2. Chow, K.; Tong, H.H.Y.; Lum, S.; Chow, A.H.L. Engineering of pharmaceutical materials: An industrial perspective. *J. Pharm. Sci.* **2010**, *97*, 2855–2877. [CrossRef]
3. Wang, J.; Fei, L.; Lakerveld, R. Process intensification for pharmaceutical crystallization. *Chem. Eng. Process. Process Intensif.* **2018**, *127*, 111–126. [CrossRef]
4. Hatcher, L.E.; Li, W.; Payne, P.; Rielly, C.D.; Wilson, C.C. Tuning Morphology in APIs: Controlling the Crystal Habit of Lovastatin through Solvent Choice and Non-Size-Matched Polymer Additives. *Cryst. Growth Des.* **2020**, *20*, 5854–5862. [CrossRef]
5. Lynch, A.; Verma, V.; Zeglinski, J.; Bannigan, P.; Rasmuson, A. Face indexing and shape analysis of salicylamide crystals grown in different solvents. *Crystengcomm* **2019**, *21*, 2648–2659. [CrossRef]
6. Li, J.; Jin, S.H.; Lan, G.C.; Xu, Z.S.; Wu, N.N.; Chen, S.S.; Li, L.J. The effect of solution conditions on the crystal morphology of beta-HMX by molecular dynamics simulations. *J. Cryst. Growth* **2019**, *507*, 38–45. [CrossRef]
7. Soper, E.M.; Penchev, R.Y.; Todd, S.M.; Eckert, F.; Meunier, M. Quantifying the effect of solvent on the morphology of organic crystals using a statistical thermodynamics approach. *J. Cryst. Growth* **2022**, *591*, 126712. [CrossRef]

8. Zhao, K.; Liu, P.; Li, K.; Zhang, Y.; Cao, J.; Cheng, J.; Yang, C. Effect of polyethylene glycol additives on the polymorph and crystal habit of carbamazepine. *J. Cryst. Growth* **2022**, *588*, 126644. [CrossRef]

9. Davey, W.P. Crystal Growth. H. E. Buckley. New York: Wiley; London: Chapman & Hall, 1951. 571 pp. $9.00. *Science* **1951**, *113*, 533.

10. Wu, H.; Wang, J.; Li, F.; Liu, Q.; Hao, H. Investigations on growth intensification of p-toluamide crystals based on growth rate analysis and molecular simulation. *CrystEngComm* **2019**, *21*, 5519–5525. [CrossRef]

11. Zhang, L.; Yan, M.; Yin, W.L.; Li, J.S.; Liu, Y.; Zhao, S.; Huang, S.L. Experimental Study of the Crystal Habit of High Explosive Octahydro-1,3,5,7-tetranitro-1,3,5,7-tetrazocine (HMX) in Acetone and Dimethyl Sulfoxide. *Cryst. Growth Des.* **2020**, *20*, 6622–6628. [CrossRef]

12. Nguyen, T.T.; Rosbottom, I.; Marziano, I.; Hammond, R.B.; Roberts, K.J. Crystal Morphology and Interfacial Stability of RS-Ibuprofen in Relation to Its Molecular and Synthonic Structure. *Cryst. Growth Des.* **2017**, *17*, 3088–3099. [CrossRef]

13. Shim, H.M.; Kim, H.S.; Koo, K.K. Molecular Modeling on Supersaturation-Dependent Growth Habit of 1, 1-Diamino-2, 2-dinitroethylene. *Cryst. Growth Des.* **2015**, *15*, 1833–1842. [CrossRef]

14. Civati, F.; O'Malley, C.; Erxleben, A.; McArdle, P. Factors Controlling Persistent Needle Crystal Growth: The Importance of Dominant One-Dimensional Secondary Bonding, Stacked Structures, and van der Waals Contact. *Cryst. Growth Des.* **2021**, *21*, 3449–3460. [CrossRef] [PubMed]

15. Liu, Y.; Black, J.F.B.; Boon, K.F.; Cruz-Cabeza, A.J.; Davey, R.J.; Dowling, R.J.; George, N.; Hutchinson, A.; Montis, R. When Crystals Do Not Grow: The Growth Dead Zone. *Cryst. Growth Des.* **2019**, *19*, 4579–4587. [CrossRef]

16. Derdour, L.; Skliar, D. Crystallization from Solutions Containing Multiple Conformers. 1. Modeling of Crystal Growth and Supersaturation. *Cryst. Growth Des.* **2012**, *12*, 5180–5187. [CrossRef]

17. Zhao, Q.; Liu, N.; Wang, B.; Wang, W. A study of solvent selectivity on the crystal morphology of FOX-7 via a modified attachment energy model. *RSC Adv.* **2016**, *6*, 59784–59793. [CrossRef]

18. Zhang, C.; Ji, C.; Li, H.; Zhou, Y.; Xu, J.; Xu, R.; Li, J.; Luo, Y. Occupancy model for predicting the crystal morphologies influenced by solvents and temperature, and its application to nitroamine explosives. *Cryst. Growth Des.* **2013**, *13*, 282–290. [CrossRef]

19. Ji, X.; Wang, J.; Wang, T.; Huang, X.; Li, X.; Wang, N.; Huang, Y.; Li, R.; Zhao, B.; Zhang, T. Understanding the role of solvent in regulating the crystal habit. *CrystEngComm* **2022**, *24*, 2226–2240. [CrossRef]

20. Wu, H.; Wang, J.; Liu, Q.; Zong, S.; Tian, B.; Huang, X.; Wang, T.; Yin, Q.; Hao, H. Influences and the Mechanism of Additives on Intensifying Nucleation and Growth of p-Methylacetanilide. *Cryst. Growth Des.* **2020**, *20*, 973–983. [CrossRef]

21. Song, L.; Zhao, F.Q.; Xu, S.Y.; Ju, X.H.; Ye, C.C. Crystal Morphology Prediction and Anisotropic Evolution of 1,1-Diamino-2,2-dinitroethylene (FOX-7) by Temperature Tuning. *Sci. Rep.* **2020**, *10*, 2317. [CrossRef] [PubMed]

22. Liu, Y.; Niu, S.; Lai, W.; Yu, T.; Ma, Y.; Gao, H.; Zhao, F.; Ge, Z. Crystal morphology prediction of energetic materials grown from solution: Insights into the accurate calculation of attachment energies. *CrystEngComm* **2019**, *21*, 4910–4917. [CrossRef]

23. Liu, Y.; Yu, T.; Lai, W.; Ma, Y.; Cao, Y.; Liu, N.; Ge, Z.; Zhao, F. Deciphering Solvent Effect on Crystal Growth of Energetic Materials for Accurate Morphology Prediction. *Cryst. Growth Des.* **2020**, *20*, 521–524. [CrossRef]

24. Horowitz, A.R.; Kontsedalov, S.; Denholm, I.; Ishaaya, I. Dynamics of insecticide resistance in Bemisia tabaci: A case study with the insect growth regulator pyriproxyfen. *Pest Manag. Sci.* **2002**, *58*, 1096. [CrossRef]

25. Nasr, H.M.; Badawy, M.E.; Rabea, E.I. Toxicity and biochemical study of two insect growth regulators, buprofezin and pyriproxyfen, on cotton leafworm Spodoptera littoralis—ScienceDirect. *Pestic. Biochem. Physiol.* **2010**, *98*, 198–205. [CrossRef]

26. Kang, G.; Kim, J.; Park, H.; Kim, T.H. Crystal structure of pyriproxyfen. *Acta Cryst. E Cryst. Commun.* **2015**, *71 Pt 8*, o588. [CrossRef]

27. Sun, H. COMPASS: An ab Initio Force-Field Optimized for Condensed-Phase Applications Overview with Details on Alkane and Benzene Compounds. *J. Phys. Chem. B* **1998**, *102*, 7338–7364. [CrossRef]

28. Li, L.; Ji, X.T.; Cheng, X.W.; Li, D.N.; Wang, T.; Huang, X.; Wang, N.; Yin, Q.X.; Hao, H.X. Effect of the solvent on the morphology of sulfamerazine crystals and its molecular mechanism. *Crystengcomm* **2022**, *24*, 5497–5506. [CrossRef]

29. McGregor, L.; Rychkov, D.A.; Coster, P.L.; Day, S.; Drebushchak, V.A.; Achkasov, A.F.; Nichol, G.S.; Pulham, C.R.; Boldyreva, E.V. A new polymorph of metacetamol. *Crystengcomm* **2015**, *17*, 6183–6192. [CrossRef]

30. Chai, S.; Li, E.; Zhang, L.; Du, J.; Meng, Q. Crystallization solvent design based on a new quantitative prediction model of crystal morphology. *AIChE J.* **2022**, *68*, e17499. [CrossRef]

31. Gupta, K.M.; Yin, Y.; Poornachary, S.K.; Chow, P.S. Atomistic Simulation To Understand Anisotropic Growth Behavior of Naproxen Crystal in the Presence of Polymeric Additives. *Cryst. Growth Des.* **2019**, *19*, 3768–3776. [CrossRef]

32. Liu, Y.; Yu, T.; Lai, W.; Ma, Y.; Kang, Y.; Ge, Z. Adsorption behavior of acetone solvent at the HMX crystal faces: A molecular dynamics study. *J. Mol. Graph. Model.* **2017**, *74*, 38. [CrossRef]

33. Ning, L.; Li, Y.; Zeman, S.; Shu, Y.; Wang, W. Crystal morphology of 3,4-bis(3-nitrofurazan-4-yl)furoxan (DNTF) in a solvent system: Molecular dynamics simulation and sensitivity study. *Crystengcomm* **2016**, *18*, 2843–2851.